SAND2014-16773C

LARGER SIZED WIRE ARRAYS ON 1.7 MA Z-PINCH GENERATOR

A.S. Safronova, V. L. Kantsyrev, M.E. Weller, V. V. Shlyaptseva, I. Shrestha, A.A. Esaulov, A. Stafford

University of Nevada, Reno, NV, USA

A. S. Chuvatin

Ecole Polytechnique, Palaiseau, France

C.A. Coverdale and B. Jones

Sandia National Laboratories, Albuquerque, NM, USA*

9th International Conference on Dense Z-pinches (DZP2014)
(Napa, California, August 3-7, 2014)

**Sandia National Laboratories is a multi-program laboratory managed and operated by Sandia Corporation, a wholly owned subsidiary of Lockheed Martin Corporation, for the U. S. Department of Energy's National Security Administration under contract DE-AC04-94AL85000*

Sandia National Laboratories

From multi-planar wire arrays at 1 MA* to larger sized at 1.7MA on Zebra

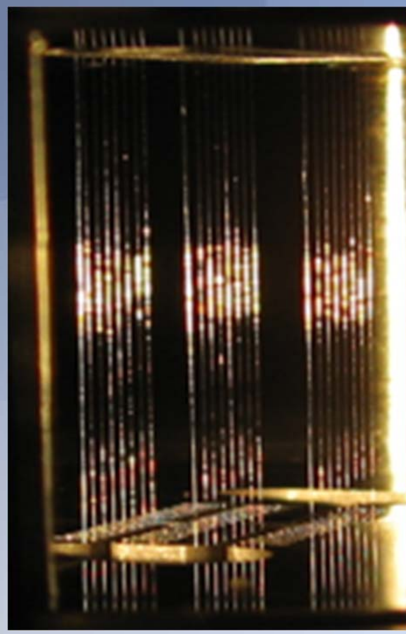

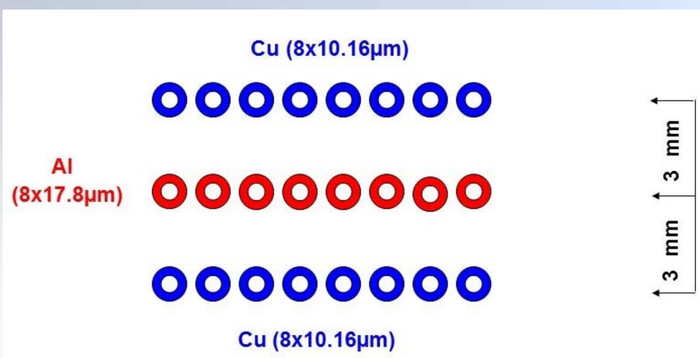

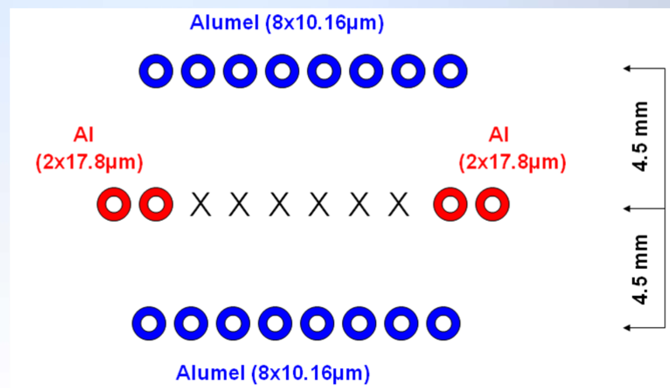

*New approach to study radiation from mixed multi-planar wire arrays was suggested, see A.S. Safronova *et al,* Physics of Plasmas 21, 031205 (2014)

MOTIVATION

Experiments on Zebra at higher current of 1.5-1.7 MA allow the implosion of larger size wire array loads than was possible with the standard current of 1 MA

Why to study the large sized planar wire arrays*?

a) Enhanced energy coupling to plasmas
b) Better diagnostic access to observable plasma regions
c) More complex planar wire load configuration with different design of the central plane

d) New application to radiation physics (how mixture radiate)?
e) New study of high-temperature precursor formation?
f) New application to jet formations for laboratory astrophysics?

*Large diameter nested stainless steel wire arrays have been studied at SNL by Christine Coverdale *et al*, PoP 15, 023107 (2008), Brent Jones *et al*, PoP 15, 122703 (2008) and by David Ampleford *et al* (2009) as well as nested copper wire arrays.

Motivation: changing global magnetic field configuration by introducing an inner plane

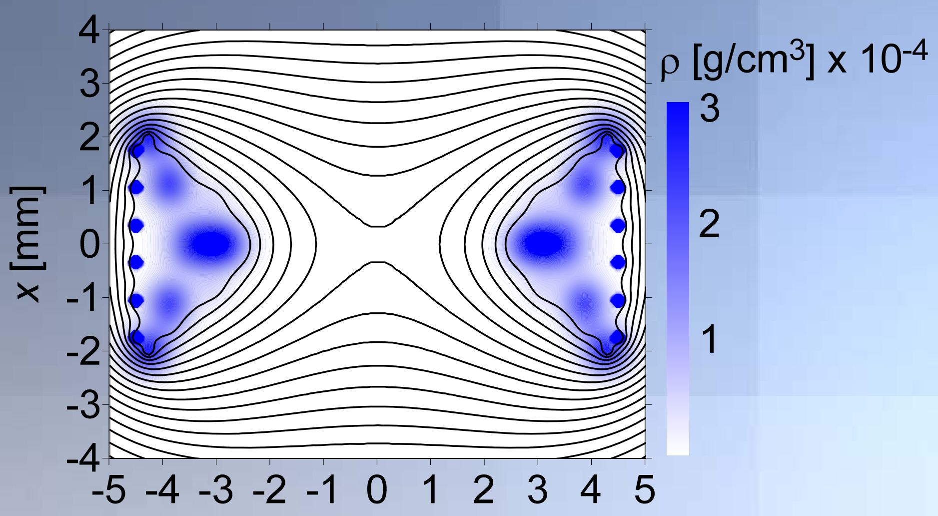

D = 9 mm DPWA

at *t* = 68 ns

Global magnetic field reconnects the array center and prevents jets formation*

*** K. M. Williamson *et al*, Phys. Plasmas 17, 112705 (2010).**

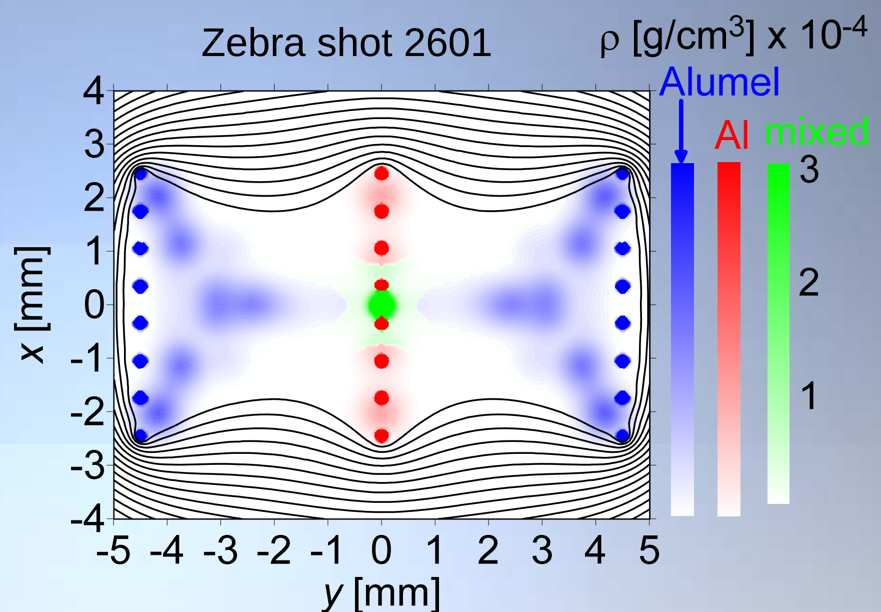

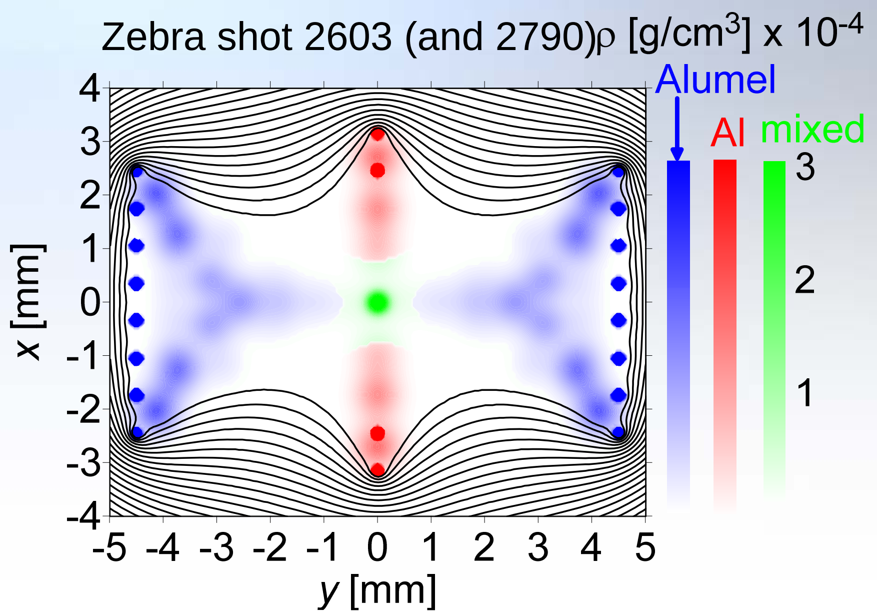

Experiments with LCM and Diagnostics setup on Zebra*

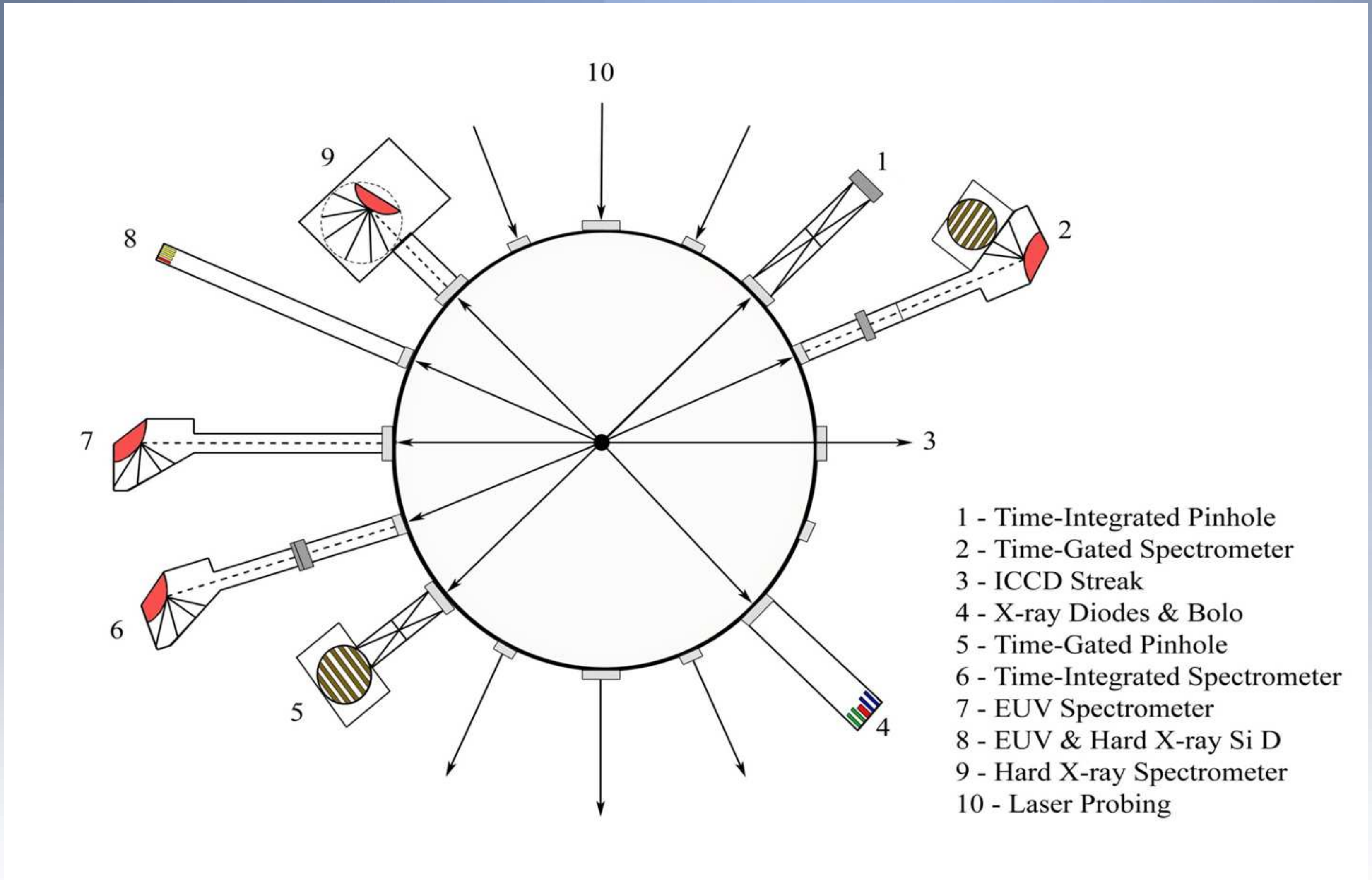

*For more about experiments with PWAs w/o and with LCM on Zebra, see V.L. Kantsyrev *et al,* High Energy Density Physics 5, 115 (2009) and Physics of Plasmas 21, 031204 (2014) and at this conference

New load design: the same number of wires but the modified central plane with different numbers of empty slots and Al wire diameters

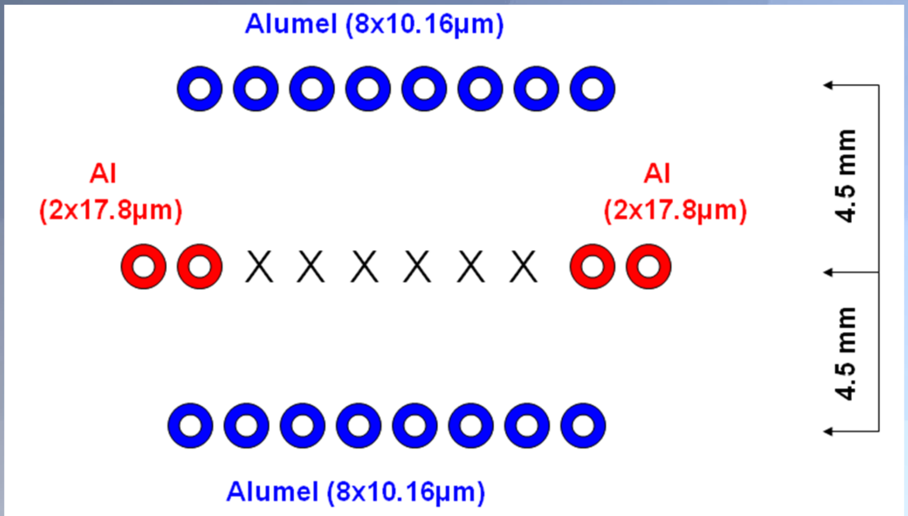

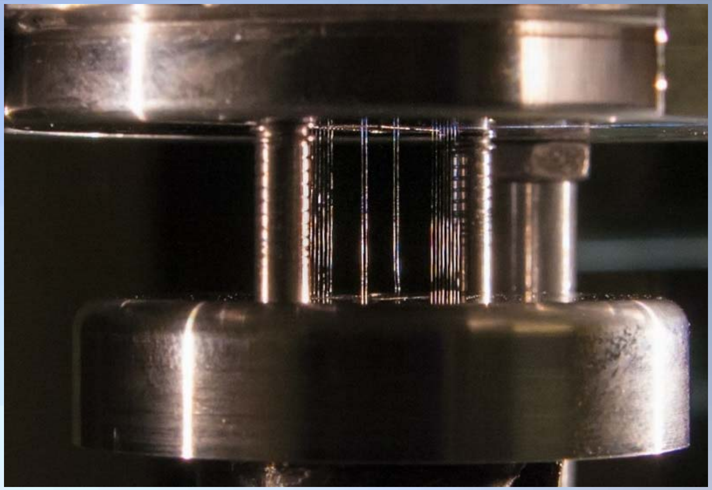

Outer row gap d=9 mm. Central row gap g=4.9 mm (6 empty slots). M=140 µg.

Zebra shot N	t_{impl}(ns)	E_{bolo}(kJ)	Current (MA)
2789	102	22.3	1.46
2790	98	27.5	1.43
3103	93	17.9	1.53
3105	99	22.1	1.66

Better diagnostic access to observable plasma regions:

Laser shadowgraphy images for Zebra shot 2790 and WADM modeling

WADM simulation

t = 60 ns

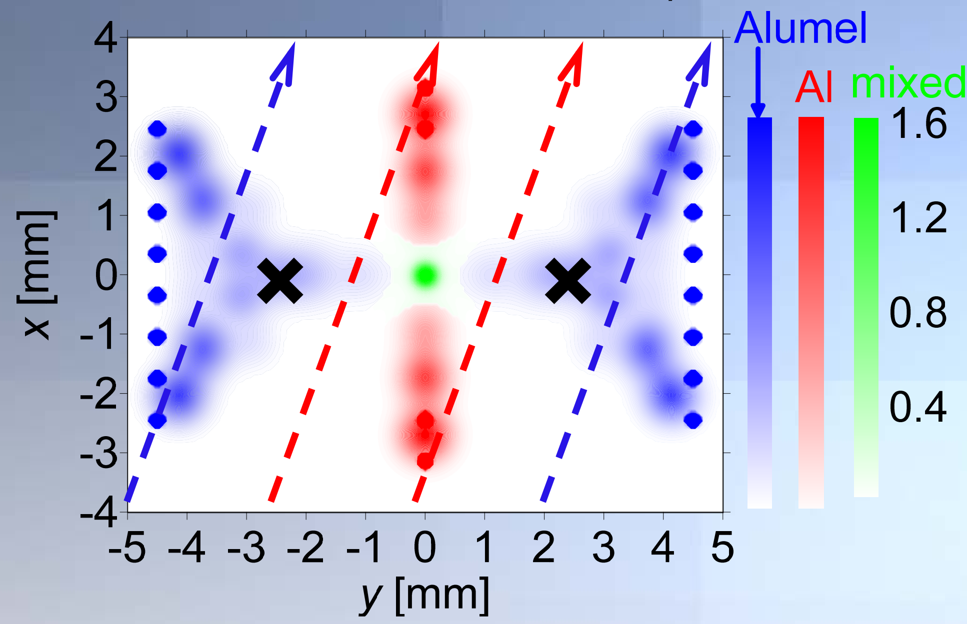

Shadowgraphy

t = 54 ns

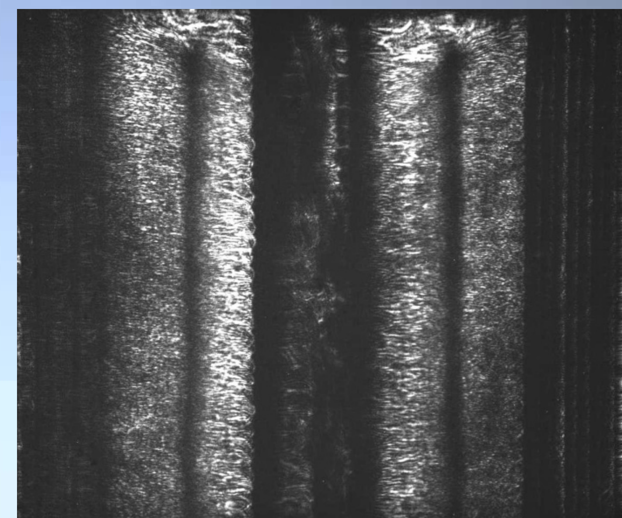

t = 61 ns

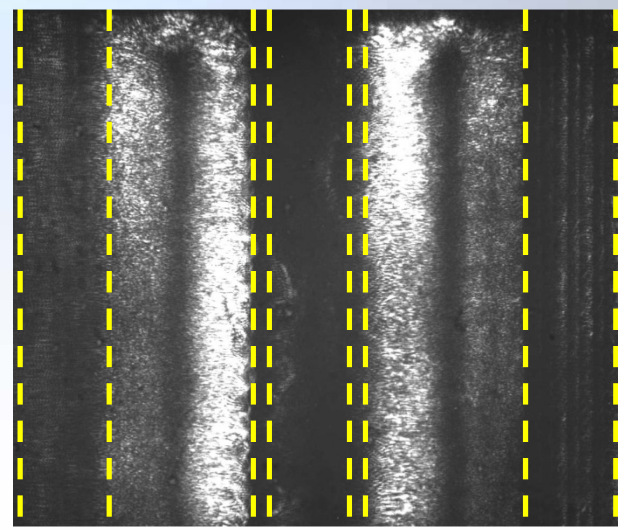

Dotted arrow lines show the direction of optical laser probing. Column-like structure between wire planes on the laser shadow images are likely the *standing shocks* that change the direction of ablated plasma flows (marked by black crosses on the above map)

Yellow dotted lines show the initial positions of wires →

TPWA Alumel/Al/Alumel: formation of the standing shocks at -60 ns before the peak of the XRD signal

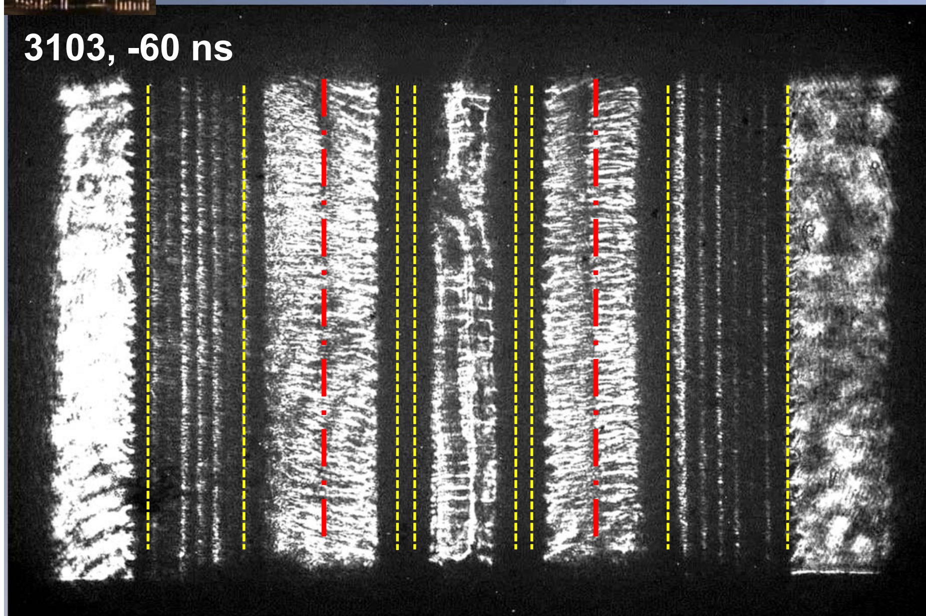

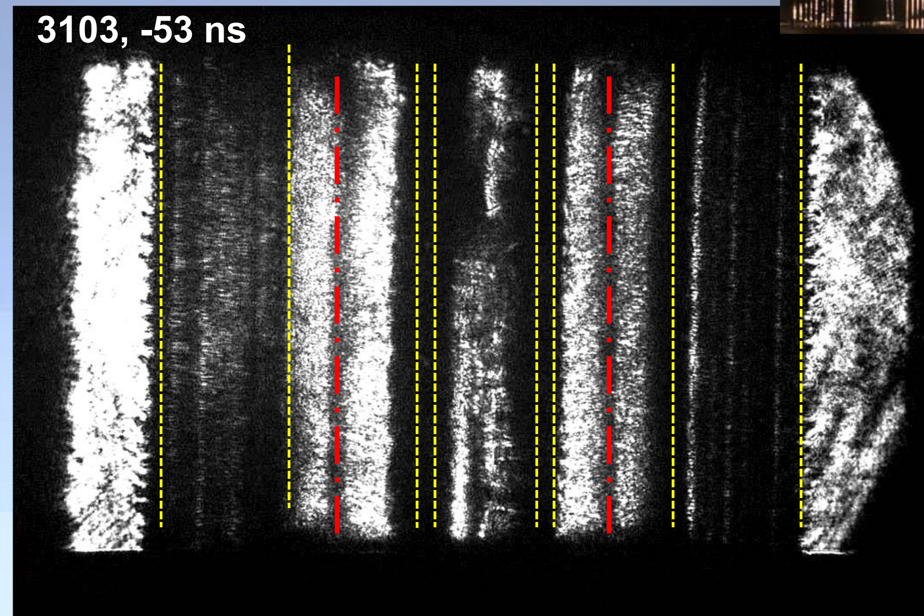

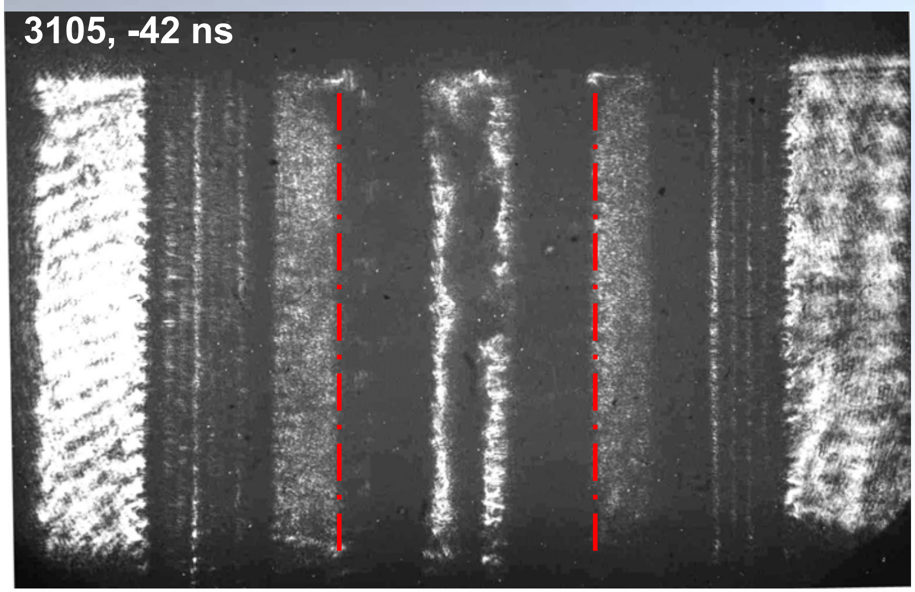

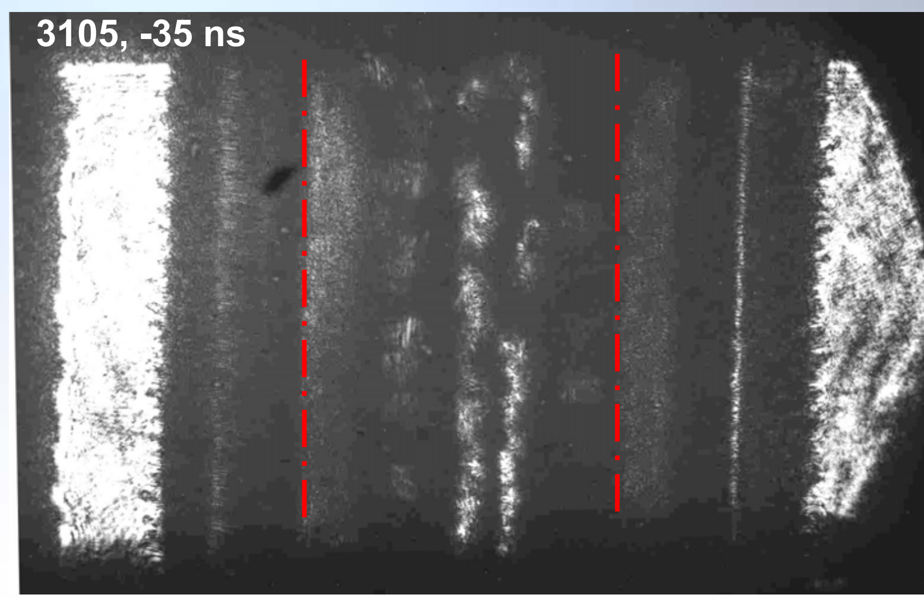

Anode is at the top for all images. AC gap is 1 cm. Time is from the peak of the XRD signal (X-ray burst).

Increasing the Al central row gap (the number of empty slots) and also increasing the outer row gap

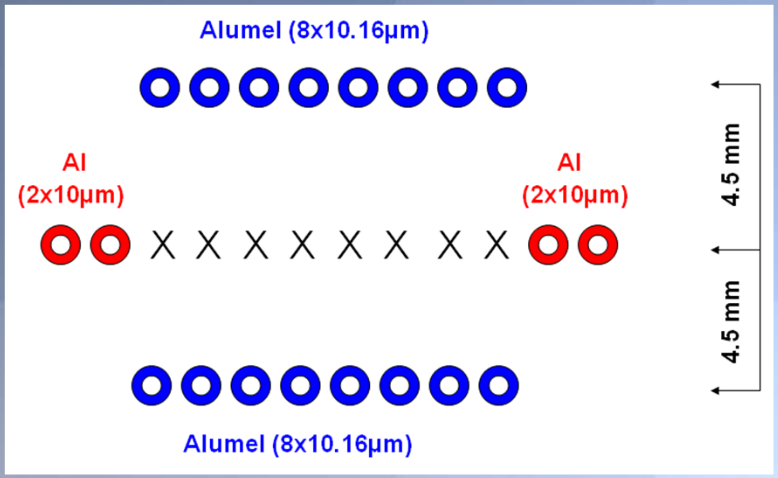

Zebra shots 2791 and 2792. Outer row gap d=9 mm. Central row gap g=6.3 mm (8 empty slots). M=120 µg.

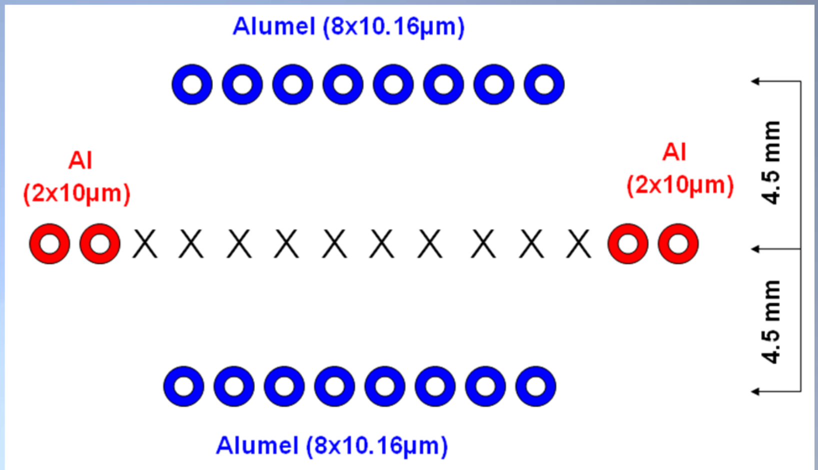

Zebra shot 2793. Outer row gap d=9 mm. Central row gap g=7.7 mm (10 empty slots). M=120 µg.

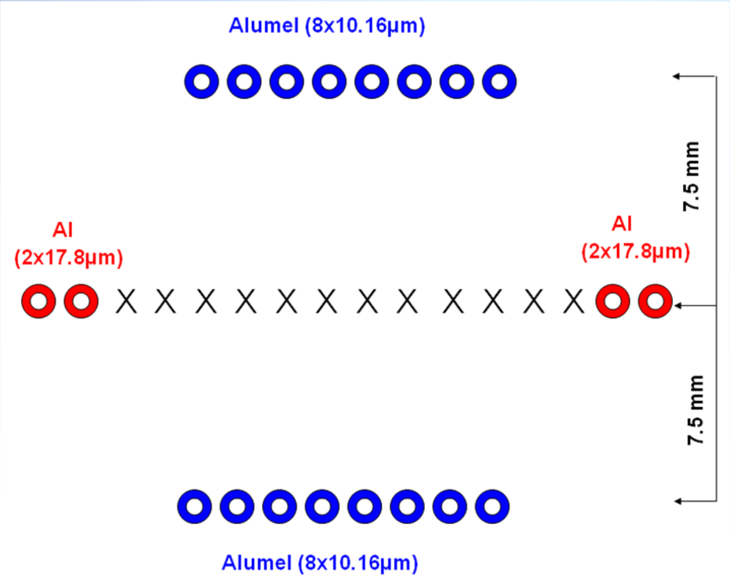

Zebra shot 2990. Outer row gap d=15 mm. Central row gap g=9.1 mm (12 empty slots). M=140 µg.

Searching for hot precursor from Planar Wire Arrays:

X-ray time-gated pinhole images and spectra together with PCD and XRD signals used for spectroscopic analysis (shot 2791)

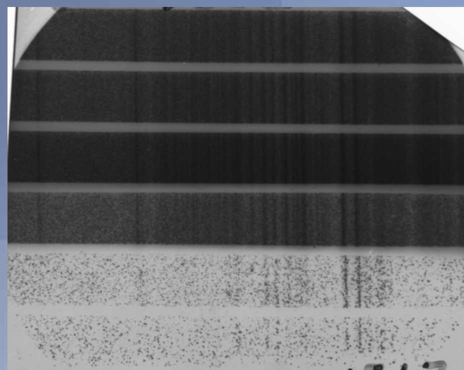

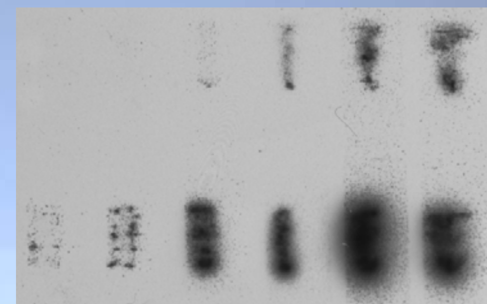

d = 9 mm (TPWA)
LCM, shot 2791
E_{bolo}=29.8 kJ
t_{imp}I=107 ns
E_{PCD}= 0.65 kJ/cm

d = 9 mm (TPWA)
LCM, shot 2601
E_{PCD}= 0.69 kJ/cm

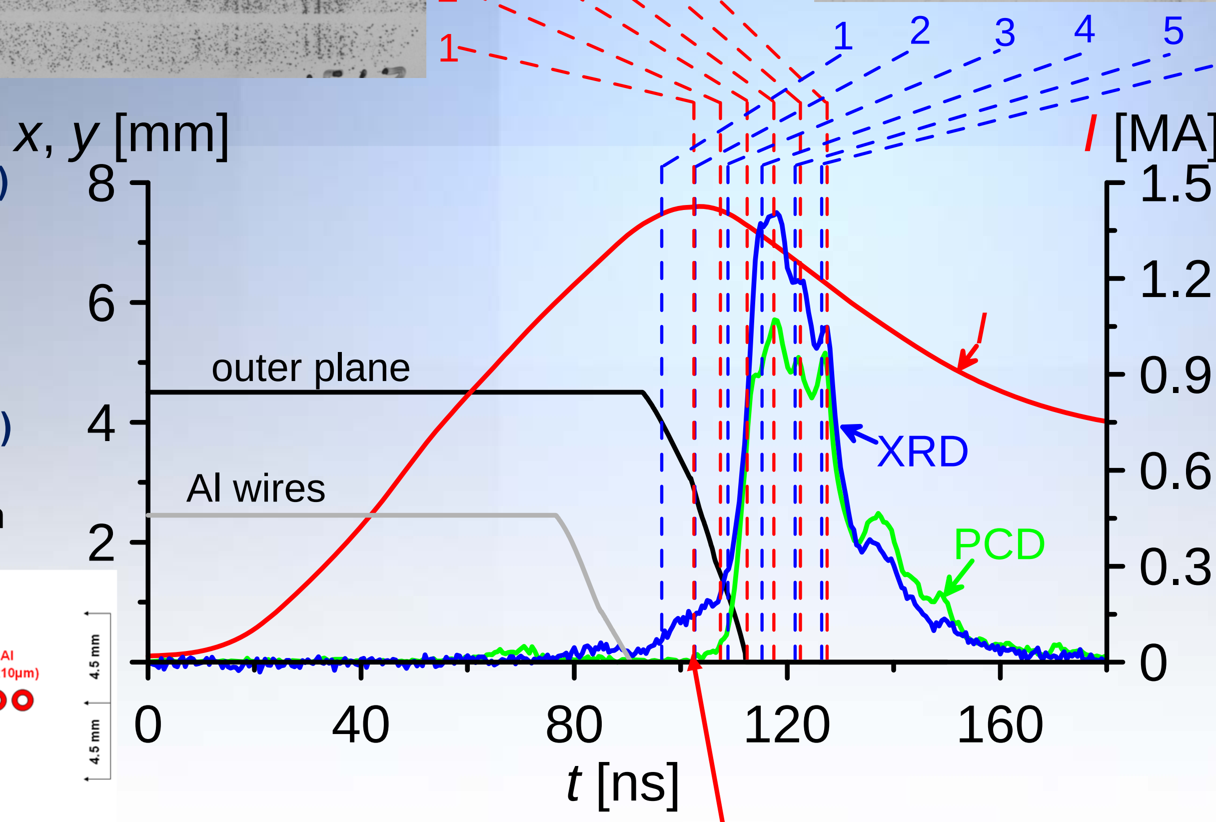

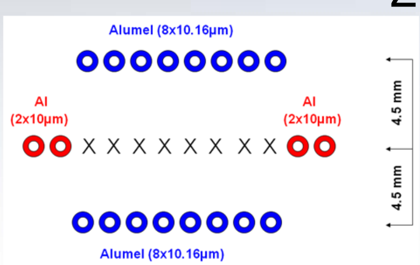

Compare to:

d = 6 mm (TPWA)
w/o LCM, shot 2316
E_{PCD}= 0.24 kJ/cm

d = 6 mm (DPWA)
w/o LCM, shot 1774
E_{PCD}= 0.12 kJ/cm

d = 3 mm (DPWA)
w/o LCM, shot 2327
E_{PCD}= 0.18 kJ/cm

L-shell Ni spectra appear at the XRD prepulse, before PCD signal, which correlates with intense double columns on x-ray pinhole image (note: we did not observe radiating double columns from PWAs before)

First observation of K-shell Al and L-shell Ni emissions before the main x-ray burst for Planar Wire Arrays (TPWA, shot 2791)

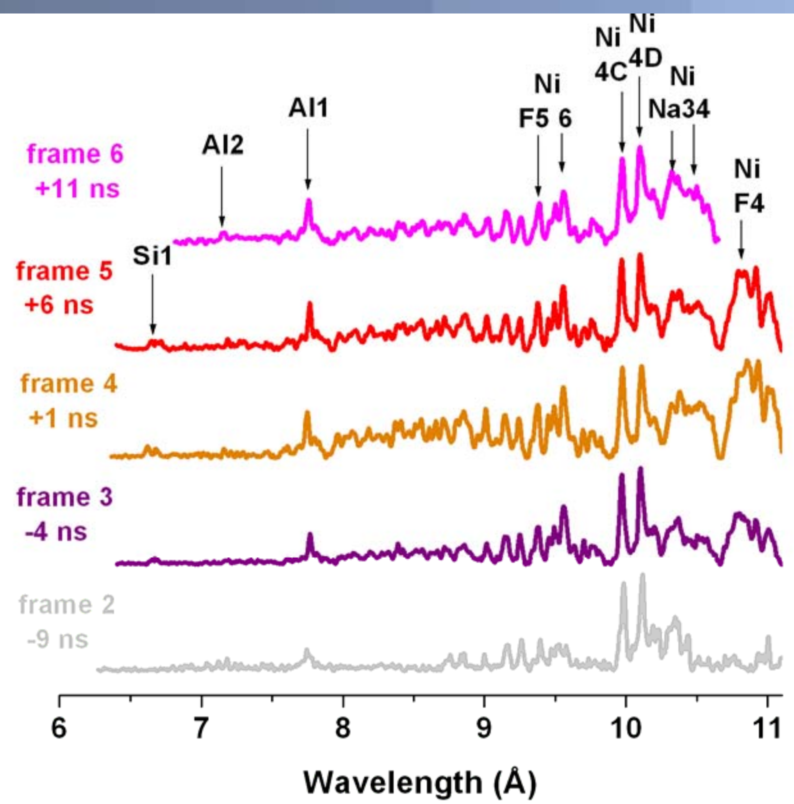

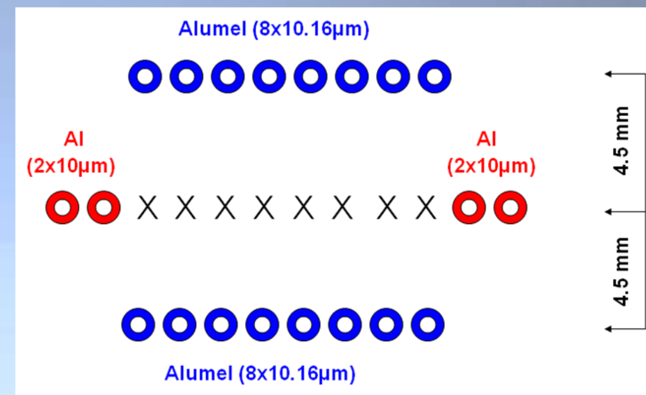

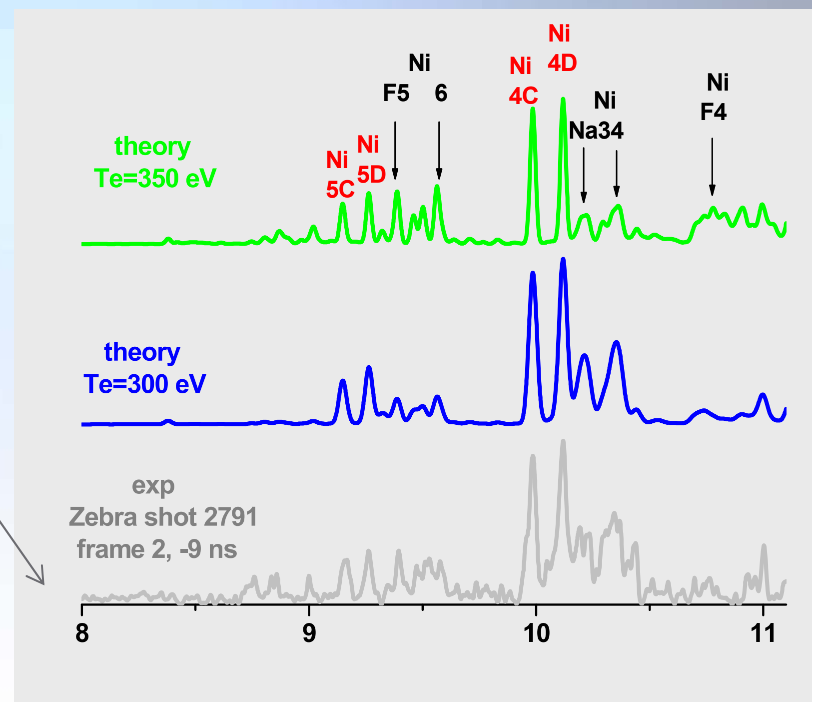

For more about Alumel PWAs, see A.S. Safronova *et al*, High Energy Density Physics 7, 252 (2011)

Increasing the Al central row gap (more empty slots). How will it influence precursor formation and K-shell Al radiation?

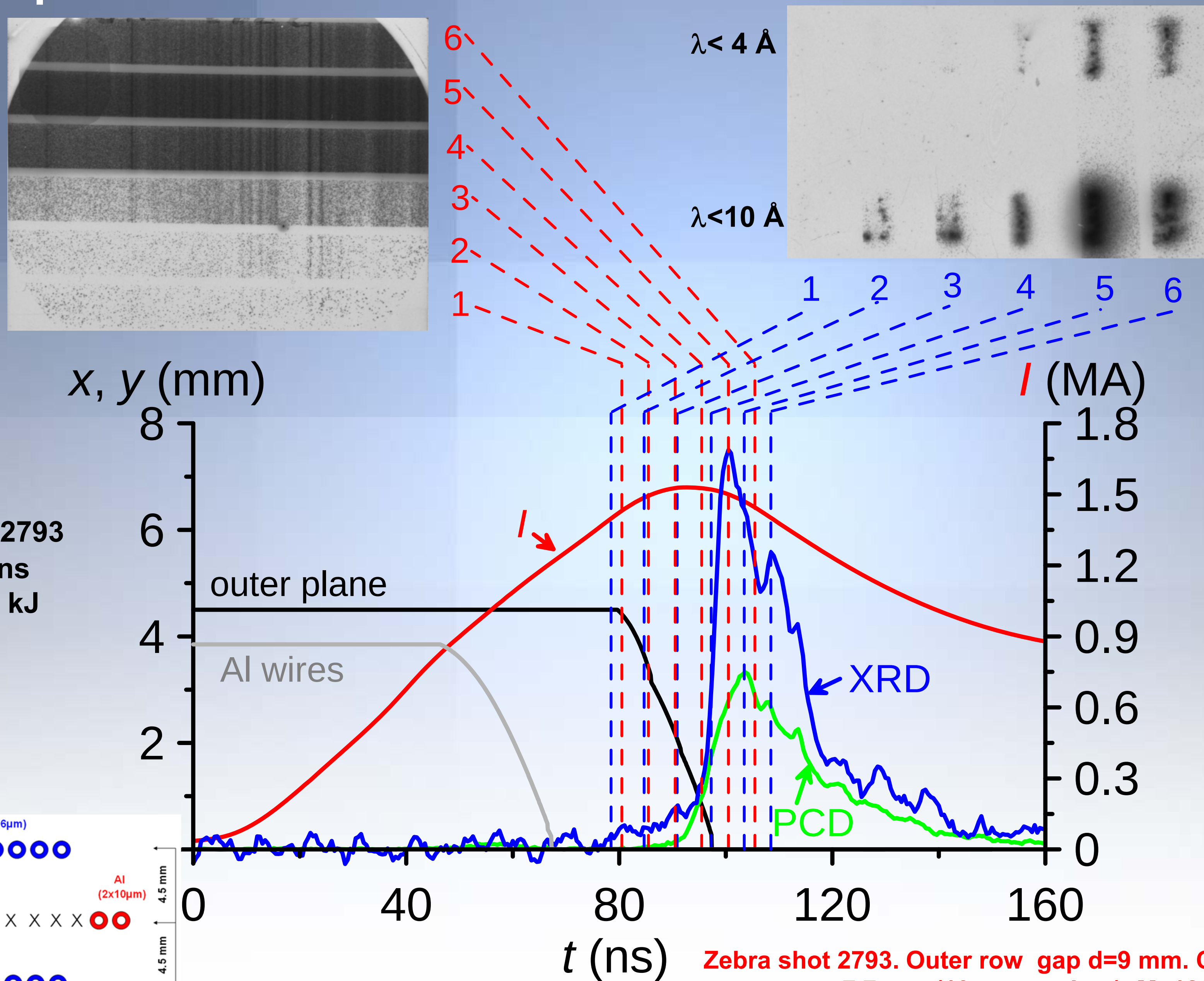

Zebra shot 2793
t_{impl}= 100 ns
E_{bolo}=30.8 kJ
I=1.5 MA
$h_{A\text{-}C}$=1 cm

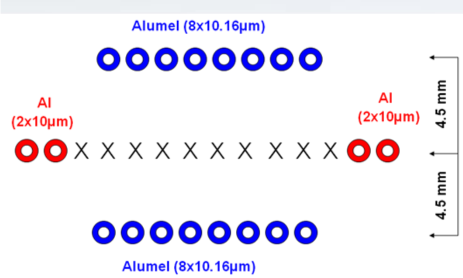

Zebra shot 2793. Outer row gap d=9 mm. Central row gap g=7.7 mm (10 empty slots). M=120 μg.

Spectroscopic analysis of time-gated spectra from shot 2793 (d=9mm and g=7.7 mm)

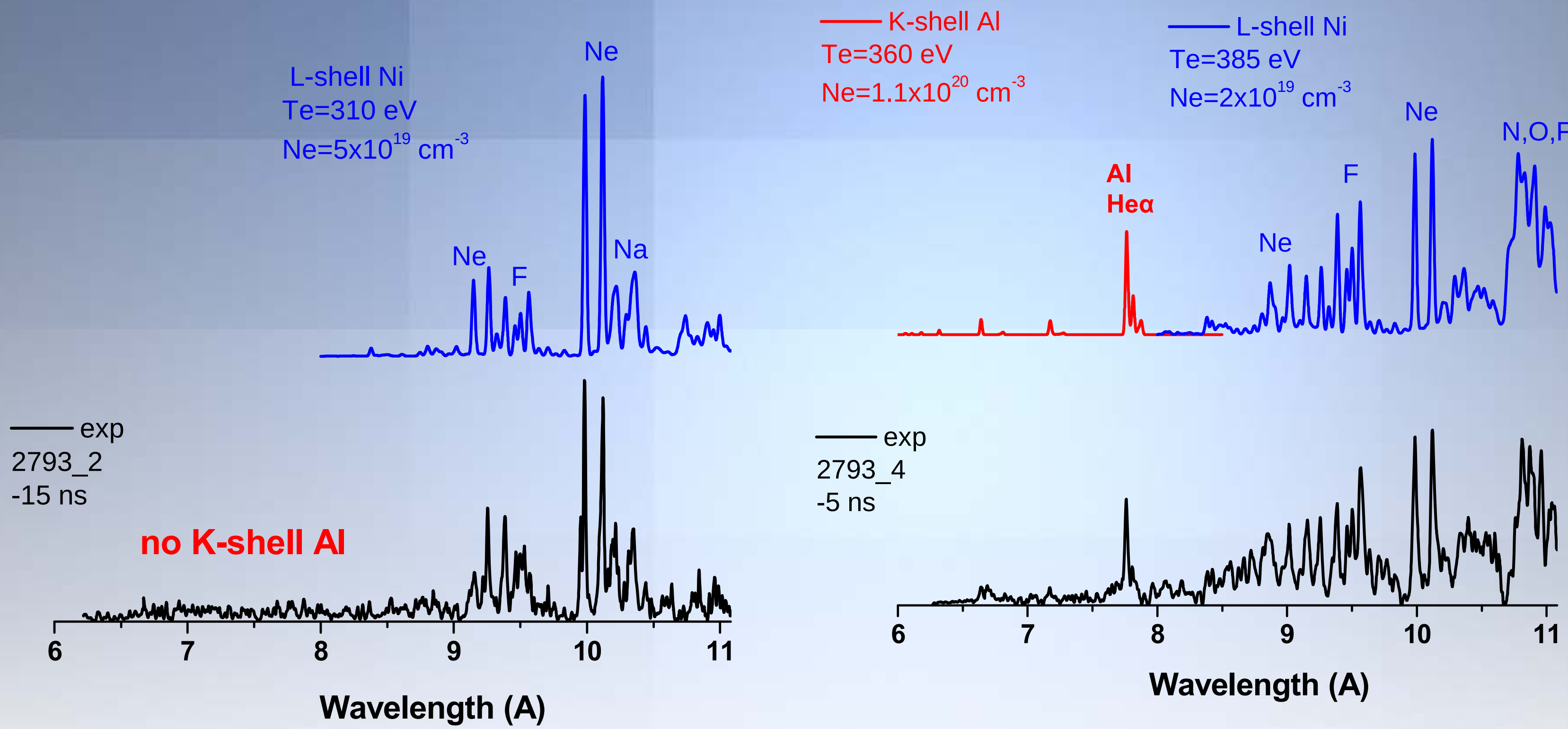

Frame 2 at -15 ns: no K-shell lines and relatively cold L-shell Ni (Na-like line structures of the same intensity as F-like ones). Frame 3 at -10 ns: appearance of Heα Al line which manifests relatively cold K-shell Al (< 300 eV). From frame 4 at -5 ns to frame 5 at the XRD peak: Te of K-shell Al plasma increases from 360 eV to 450 eV (prominent H-like Lyα Al line) and so does of L-shell Ni plasmas reaching its maximum value among all considered TPWA shots (very intense N, O, F peak).

Further increasing the Al central row gap (more empty slots) and also increasing the outer row gap. How will it influence precursor formation and K-shell Al and L-shell Ni radiation?

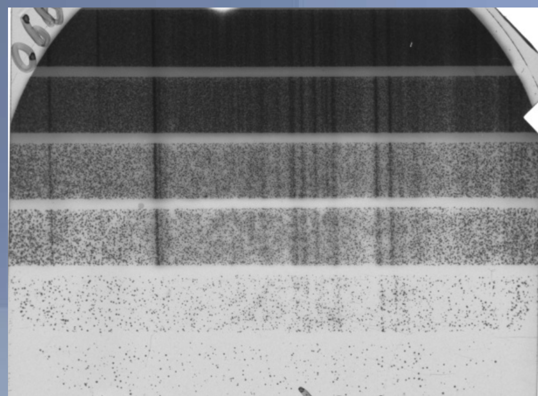

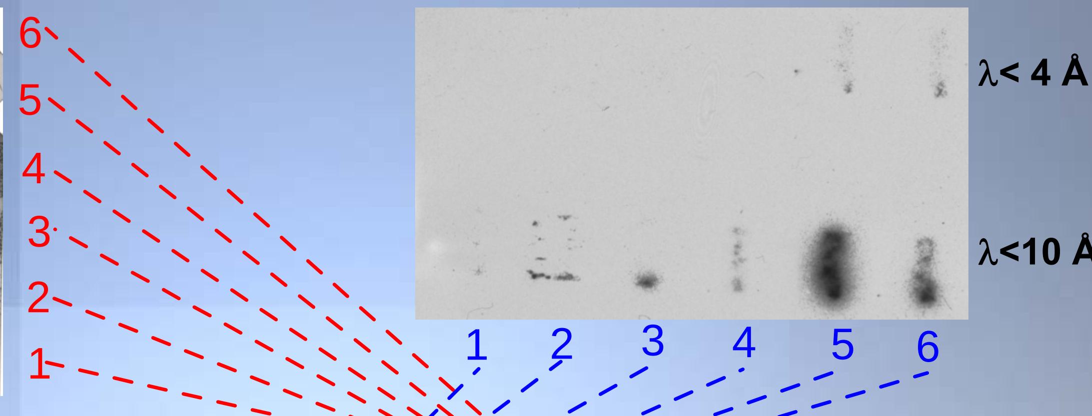

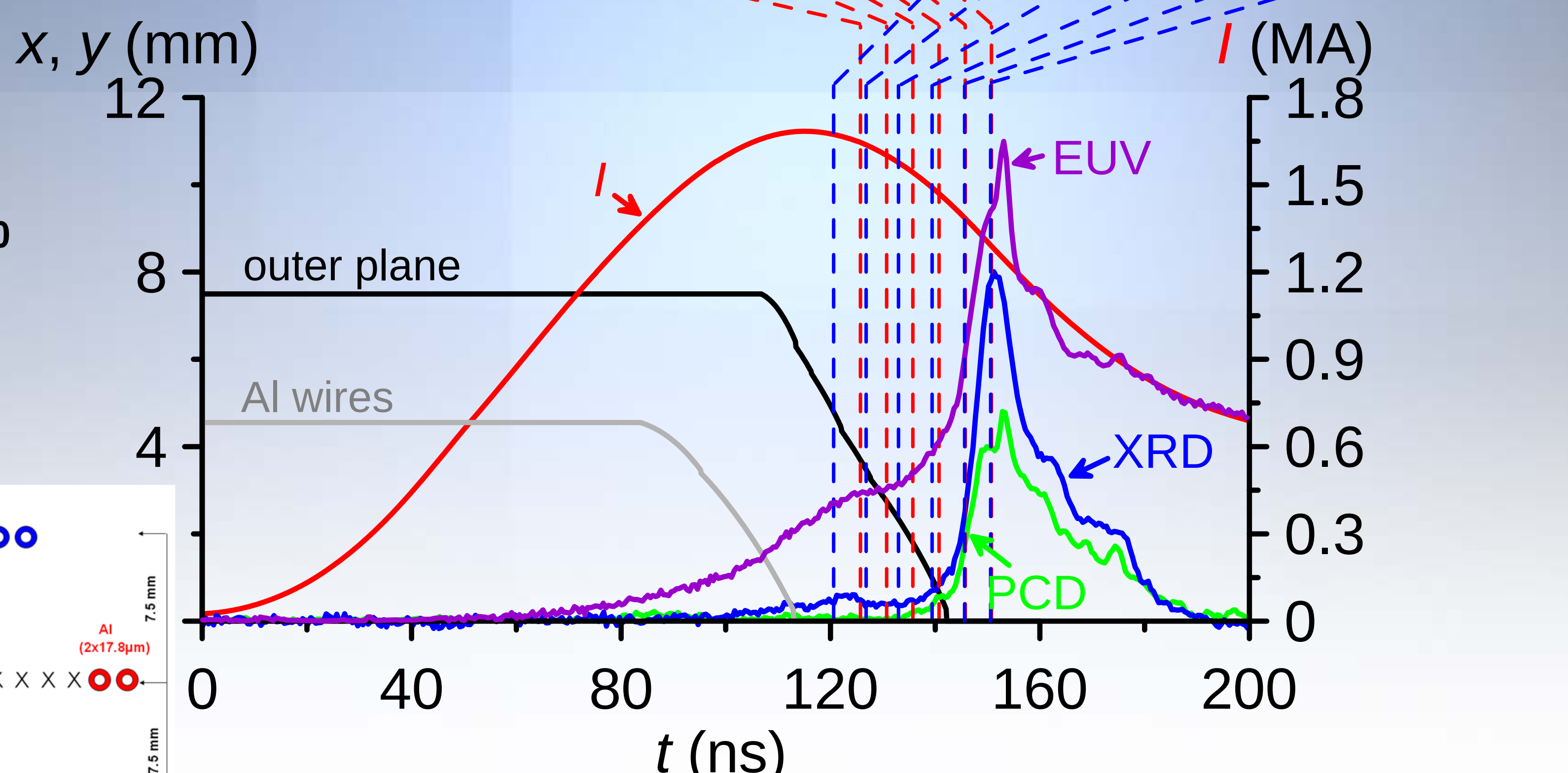

Zebra shot 2990

t_{impl}= 135 ns

E_{bolo}=25.4 kJ

I=1.67 MA

h_{A-C}=1 cm

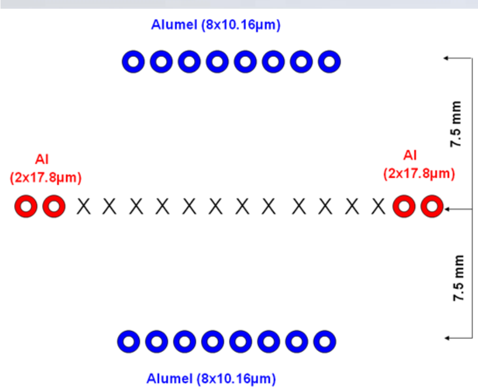

Zebra shot 2990. Outer row gap d=15 mm. Central row gap g=9.1 mm (12 empty slots). M=140 µg.

Spectroscopic analysis of time-gated spectra from shot 2990 (d=15 mm and g=9.1mm)

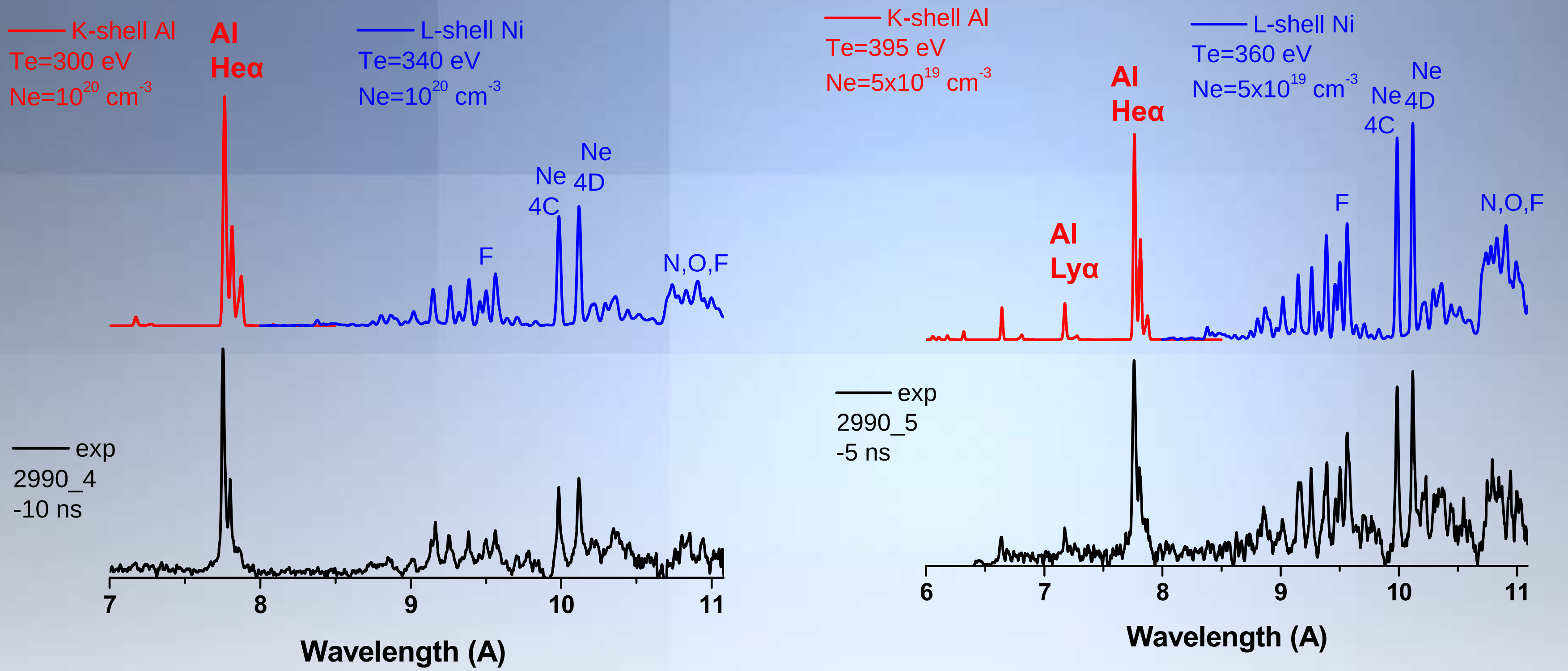

Frame 2 at -20 ns: no K-shell lines and relatively cold L-shell Ni (Na-like line structures of the same intensity as F-like ones). Frame 3 at -15 ns and frame 4 at -10 ns: appearance of Heα Al line which manifests relatively cold K-shell Al (< 300 eV). From frame 5 at -5 ns to frame 6 at the XRD peak: Te of K-shell Al plasma increases from 395 eV to 505 eV which is the maximum value among all considered TPWA shots. Te of L-shell Ni plasmas is between 340 and 360 eV for most of the observed time which is lower than for shot 2793 and reaches its maximum value at the XRD peak (which is still below 400 eV).

Summary of spectroscopic comparison of time evolution of modeled electron temperatures of K-shell Al plasmas

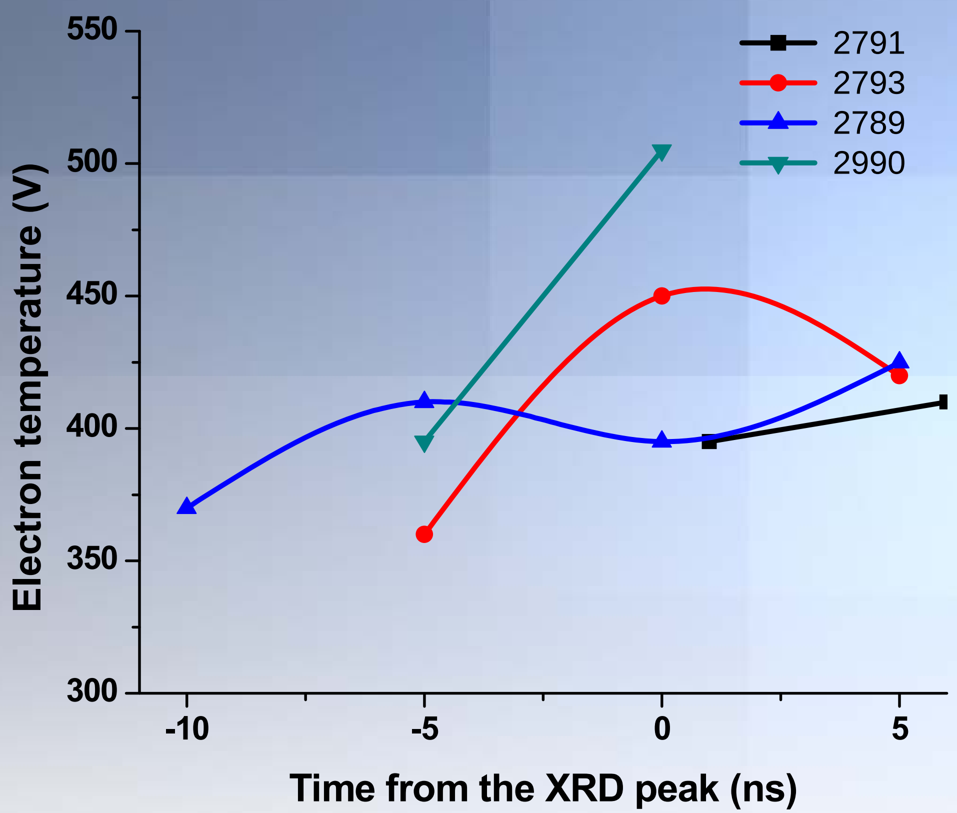

Zebra shot	Outer row gap	Central row gap	Al/Ni (%)	KE_{Al} (kJ)
2791	d=9 mm	g=6.3 mm	7.4	0.093
2793	d=9 mm	g=7.7 mm	7.4	0.107
2789	d=9 mm	g=4.9 mm	23.6	
2990	d=15 mm	g=9.1 mm	23.6	0.4

The maximum Te of 505 eV was estimated for shot 2990 (the largest central row gap)

Electron density is between $5x10^{19}$ cm^{-3} and $1.4x10^{20}$ cm^{-3}

H-like Lyα Al line (which indicates that Te ≥ 300eV) was observed as early as at -10 ns in shot 2789 but only from -5 ns (frame 4) in shot 2793 and from -5 ns (frame 5) in shot 2990

Summary of spectroscopic comparison of time evolution of K-shell Al to L-shell Ni ratio

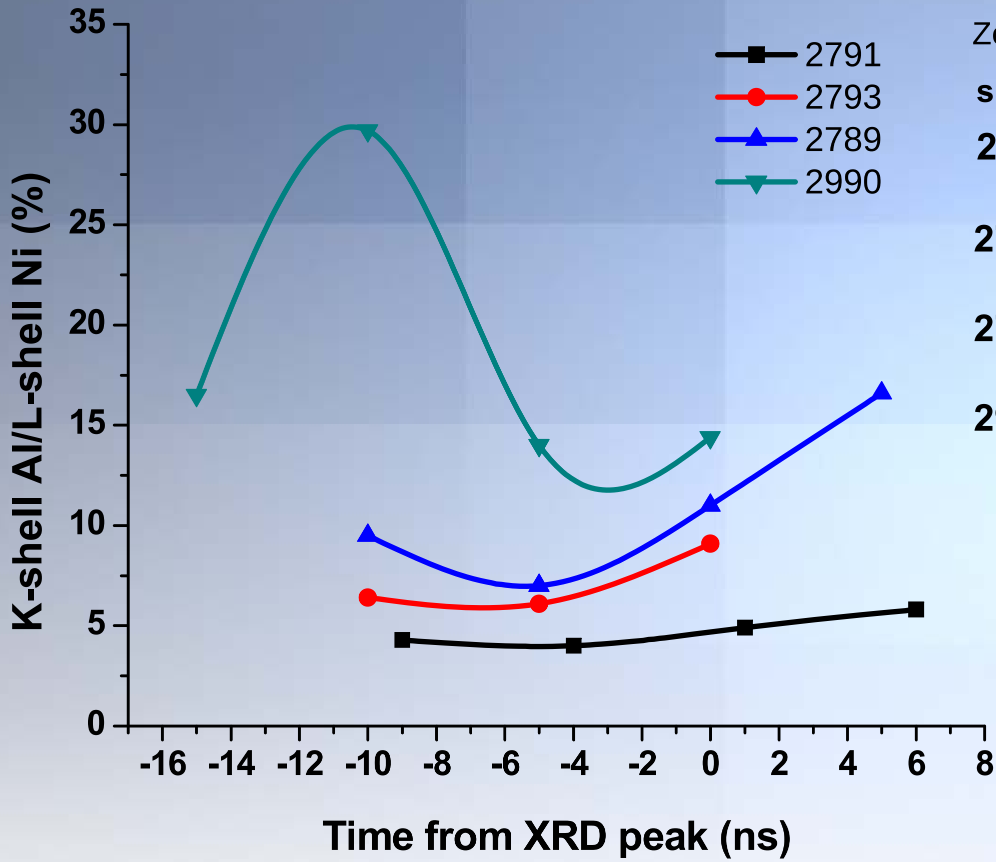

Zebra shot	Outer row gap	Central row gap	Al/Ni (%)	E_{PCD} (kJ)
2791	d=9 mm	g=6.3 mm	7.4	0.65
2793	d=9 mm	g=7.7 mm	7.4	0.73
2789	d=9 mm	g=4.9 mm	23.6	0.34
2990	d=15 mm	g=9.1 mm	23.6	0.39

The maximum ratio was estimated for shot 2990 (the largest central row gap and the largest outer row gap)

Note that time-gated spectra include all K-shell Al radiation but only part of L-shell Ni radiation, then the values on the plot above are the relative values for comparison purposes

No K-shell Al lines but prominent L-shell Ni lines on frame 2 in shot 2793 (at -15 ns) and in shot 2990 (at -20 ns)

Summary of spectroscopic comparison of time evolution of modeled electron densities of K-shell Al plasmas

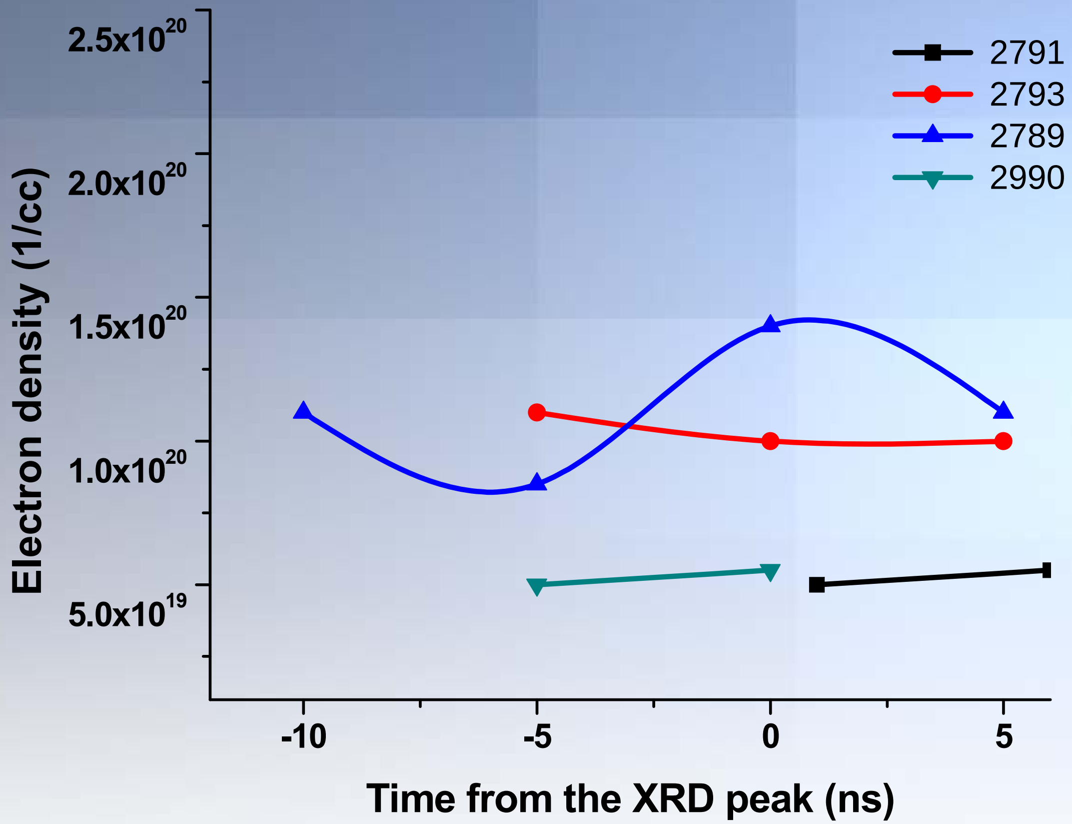

Zebra shot	Outer row gap (mm)	Central row gap (mm)	Al/Ni (%)
2791	**9**	**6.3**	**7.4**
2793	**9**	**7.7**	**7.4**
2789	**9**	**4.9**	**23.6**
2990	**15**	**9.1**	**23.6**

In general, the electron density (Ne) increases smoothly with time. Note that Ne has the largest values of about 1.5×10^{20} cm^{-3} for the shot 2789 (the smallest number of empty slots). Also the smallest values of Ne are for shots 2990 (the maximum number of empty slots) and 2791 (moderate number of empty slots).

Preliminary calculations of distribution of the current for larger size TPWA at enhanced current of 1.5 MA

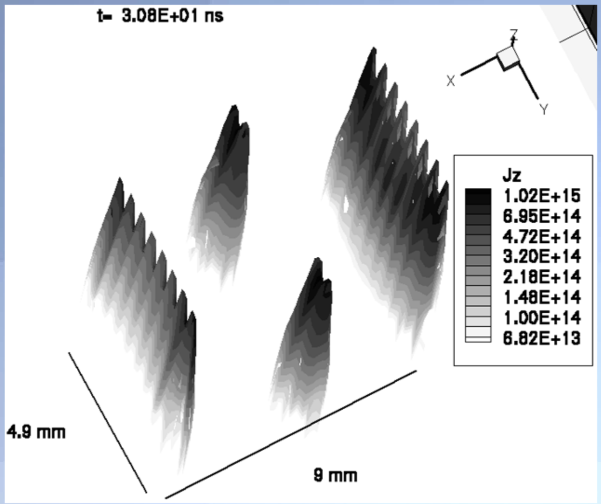

Initial position and explosion of wires

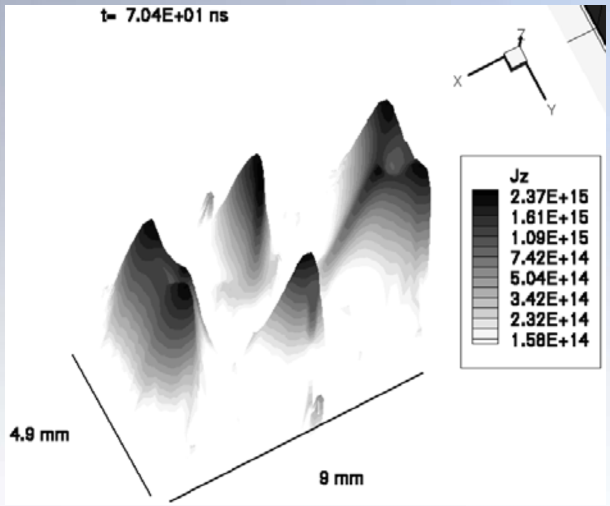

2D RMHD code developed in XY geometry by A.Chuvatin

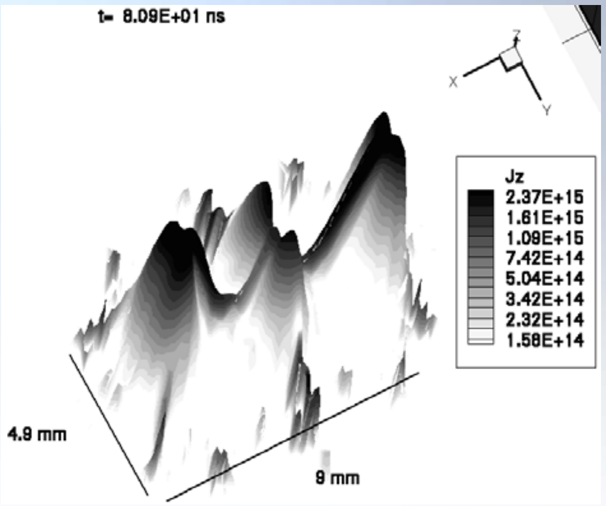

Beginning of mixture of Al with external plane mid-Z plasmas

More mixture with external plane plasmas

SUMMARY AND FUTURE WORK

- The results of new experiments with larger sized Planar Wire Arrays at enhanced current of 1.5-1.7 MA on Zebra have been presented. High linear radiation yield were measured.

- The modified Al central wire plane has different number of empty slots from N=6 up to N=12 to investigate the precursor formation and K-shell Al plasma flow. We demonstrate how the size of the gap in the middle plane influences K-shell Al radiation.

- In addition, the outer row gap between Alumel (mostly Ni) planes was increased up to d=9 mm (compared to 6 mm at standard current) and even further up to 15 mm along with increasing the number of empty slots (up to N=12) in the central plane to study effects of outer planes on precursor formation and L-shell Ni radiation.

- Comprehensive spectroscopic analysis of four shots has been accomplished that highlights the following: the maximum electron temperature of 505 eV for K-shell Al was reached in Zebra shot 2990 (max N=12, g=9.1 mm and max d=15 mm); the maximum electron temperature for L-shell Ni was for Zebra shots 2793 (N=10,g=7.7 mm and d=9 mm), and the maximum ratio of K-shell Al to L-shell Ni was also observed for the Zebra shot 2990 .

- The increased central row gap ($N \geq 10$) resulted in delay of K-shell Al compared to L-shell Ni at early times which was never observed before.

- Future work will focus on the further investigation of two different plasma flows in time and space and on the study of jet formation in two perpendicular directions for astrophysics.

ACKNOWLEDGMENTS

We would like to thank the NTF team at the UNR for their effort in Zebra operation during the experiments and help with data collection.

This work was supported by NNSA under DOE Cooperative Agreements DE-NA0001984, DE-FC52-06NA27588, DE-FC52-06NA27586 and in part by DE-NA0002075.

Sandia National Laboratories is a multiprogram laboratory managed and operated by Sandia Corporation, a wholly owned subsidiary of Lockheed Martin Corporation, for the U.S. Department of Energy's National Nuclear Security Administration under Contract No. DE-AC04-94AL85000.